ACS OMEGA

http://pubs.acs.org/journal/acsodf

Article

Utilizing Cell Culture Assisted Anodization to Fabricate Aluminium Oxide with a Gradient Microstep and Nanopore Structure

Zhiying Zhang, Yiyan Guo, Jiangbo Lu, Juan Li,* Yingjun Ma, Ting Liu, Ruiqing Liang, Runguang Sun,* and Jun Dong*

Cite This: *ACS Omega* 2022, 7, 35668−35676

Read Online

ACCESS | Metrics & More | Article Recommendations

ABSTRACT: Anodic aluminum oxide (AAO) with a gradient microstep and nanopore structure (GMNP) is fabricated by inversely using cell culture to control the reaction areas in the electrochemical anodization, which shows a larger porosity than that of typical planar AAO. The figure of the microstep is influenced by the cell dehydration temperature which controls the cell shrinkage degree. A GMNP AAO with a diameter of 2.5 cm is achieved. Polymer with a gradient microstep and nanonipple structure is fabricated using the GMNP AAO as the template, which denotes that GMNP AAO could become a broad platform for the structural preparation of various materials with advanced functions.

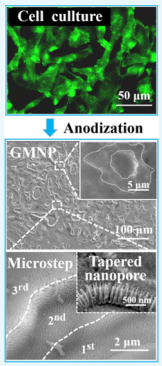

INTRODUCTION

Gradient microstep integrated with a nanostructure are nanostructures arrayed on microsteps whose heights gradually change from high to low at the microscale. Due to structural asymmetry, large specific surface area, and small solid−liquid contact area, they have promising applications in many fields, such as directional liquid self-transportation,[1−4] water collection,[5,6] catalysis,[7] tissue culture,[8,9] and so on. Furthermore, the gradually changed microstructures can prevent the nanostructures from being completely destroyed,[10] which increases the stability of the material. However, these structures are not easily achieved using the existing technologies. For example, when preparing the gradually changed microsteps by the top−down techniques (e.g., photolithography or laser etching), the previously etched surface has to be repeatedly found and aligned precisely. Also, it is always needed to integrate the nanostructures to the microstructures by sputtering or chemical bath deposition, which have poor adhesion to the substrate.[11,12] Because the nanostructures are not of the same material as the substrate, they are highly susceptible to detachment in hot and cold alternating environments due to the mismatched thermal expansion coefficients. Therefore, preparing a gradient microstep integrated with a nanostructure by a practical method is still a difficult problem to be solved.

After nearly three decades of systematic research, self-organized anodic aluminum oxide (AAO) is not only one of the most popular templates to prepare various functional nanostructures with unique optic, electric, and magnetic properties but also a versatile platform to develop novel chemical and biological sensors, energy storage, drug delivery systems, and so on.[13−17] To date, self-ordered AAO not only with wafer-scale area[18] but also with a period with 60−900 nm can be obtained in normal and novel organic acid electrolyte.[19−22] Also, the effect of the other parameters, such as anodization voltage,[22] the convex of the Al substrate[19,23] on the growth of the nanopores are also well studied. Recently, Mebed et al. used impurity aluminum as a substrate to generate alumina with three-dimensional (3D) nanopores and used the 3D AAO as a template to fabricate Ni nanowires with a larger surface area and more stable mechanical ability.[24−27] It is clear that if a feasible method can be found to obtain AAO with a gradient microstep and nanopore structure (GMNP), a viable platform is provided for the preparation of a gradient microstep integrated with a nanostructure of various materials with advanced functions. However, it should be noted that the reported structures of AAO are all isotropic axisymmetric planar arrays. This is because, using the existing electrochemical anodization technique, the entire alumina surface undergoes an undifferentiated reaction, neither chemical corrosion nor electro-

Received: June 3, 2022
Accepted: September 9, 2022
Published: September 28, 2022

© 2022 The Authors. Published by American Chemical Society

chemical growth of the alumina is anisotropic.[13] Therefore, GMNP AAO cannot be achieved.

In principle, the depth increment of AAO is the result of the dynamic balance between the generation rate and dissolved rate of the alumina film in contact with the electrolyte at the bottom of the pore (i.e., barrier layer) under the electric field.[13,28] The alumina film has a uniform depth, the essence of which is that all nanopores on the entire reaction surface react simultaneously and indiscriminately. Thus, in theory, the two-dimensional planar array structure of AAO can be unfolded in three-dimensional space and deliver a GMNP AAO, if a method can be found to separately control the reaction regions to let these regions be anodized at different times, which results in different regions having different depths. Due to the biocompatibility and controllable structural parameters, AAO has been an excellent platform for studying the effects of nanostructure parameters (e.g., porosity, pore depth) on cell growth for many years.[29−33] It was reported that the cells stayed on the top of the pore and firmly adhered to the top surface of the pore by focal adhesion.[31] In this situation, the cell body completely separates the electrolyte from the bottom of the alumina membrane. Therefore, we wonder if it is possible to inversely use the cell culture to control the contact area between the alumina membrane and the electrolyte to obtain the GMNP AAO.

Here, by combining cell culture and its dehydration process with electrochemical oxidation, the fabrication of GMNP AAO is achieved. The influence of cell culture density, cell culture time, and cell dehydration temperature on GMNP AAO morphology are systematically studied. The GMNP AAO with a diameter of 2.5 cm is achieved. Furthermore, polymer with a gradient microstep and nanonipple structure is prepared by thermal polymerization using the as-prepared GMNP AAO as a template, which demonstrates that the GMNP AAO could become a broad platform for the structural preparation of various materials with advanced functions. This method not only needs no large and expensive instruments but also can achieve large-scale preparation of GMNP AAO at a low cost.

EXPERIMENT AND METHOD

Cell Culture. All experiments were performed with the breast cancer cell, MDA-MB-231, which was purchased from the National Collection of Authenticated Cell Cultures, China. The MDA-MB-231 cells were grown in the complete medium composed of high-glucose Dulbecco's modified Eagle's medium (DMEM, Gibco), 10% fetal bovine serum (FBS, BI), and 1% penicillin/streptomycin (Gibco, China), which was placed in an incubator containing 5% CO_2 at 37 °C. Prior to seeding, all of the samples were soaked in ethanol for 5 min.

Preparation of GMNP AAO. The ordinary AAO was fabricated by typical mild anodization, where the electropolished highly pure (99.999%) aluminum disk with a diameter of 25.4 mm was anodized in 0.3 M oxalic acid at 40 V, 16 °C for 3 h. After the ordinary AAO was soaked in 75% alcohol for 5 min, the MDA-MB-231 cells were cultured on it with a fixed density (from 2×10^4 to 6×10^4 cells/cm^2) for the desired time (from 24 to 120 h) in a 9 cm glass Petri dish. After the cell culture, the ordinary AAO with cells was washed with phosphate buffer (PBS) three times, which was then soaked in 2% glutaraldehyde at room temperature for 30 min and rinsed with PBS and deionized water three times respectively to fix the adhered cells. Subsequently, the ordinary AAO with cells was anodized again in 0.3 M oxalic acid at 40 V, 16 °C for 1 h, which was called first anodization. After the cells on AAO were dehydrated at the desired temperature for 12 h, the second anodization of the AAO was conducted under the same conditions as that of the first anodization, followed by immersing the AAO in the mixed solution of 1.8 wt % chromic oxide and 6 wt % phosphoric acid at 75 °C for 3 h to chemically dissolve the alumina layer to obtain aluminum with a gradient microstep and nanodent (GMND). Finally, an AAO with a gradient microstep and nanopore (GMNP) structure can be obtained by the third anodization of aluminum with GMND with the same conditions as that of the second anodization but with a reaction time of 10 min. The AAO with a gradient microstep and tapered nanopore structure was obtained by anodizing aluminum with GMND in 0.3 M oxalic acid at 40 V, 16 °C for 25 s, followed by the pore widening treatment in 5 wt % phosphoric acid solution at 30 °C for 15 min, which was repeated five times.

Preparation of Polymer with Gradient Microstep and Nanonipple Structure. Methyl methacrylate (MMA) was purified by reducing pressure distillation to remove the inhibitor. Benzoyl peroxide (BPO), the polymerization initiator, was recrystallized in methanol to remove impurities. Then, MMA and BPO were mixed in a mass ratio of 10:0.042, and were continued to be stirred in a thermostatic water bath for prepolymerization at 80 °C. When the viscosity of the mixture was obviously increased, which stood for the formation of polymer precursor, the reaction ceased. Then, the container was immediately flushed by the running water from the outside wall to take away the heat. After cooling down to room temperature, the polymer precursor was reserved in the refrigerator at 4 °C. Then, the AAO template with a gradient microstep and tapered nanopore structure was covered on the polymer under the pressure of 111 Pa. The whole sample was cured at 50 °C for 15 h, followed by heating at 100 °C for 3 h to accomplish polymerization. After that, the Al substrate was removed by dipping the sample into a mixture solution of 0.2 M $CuCl_2$ and 10 wt % HCl. Subsequently, the sample was immersed in 10 wt % NaOH for 10 min to remove aluminum oxide. After washing with deionized water and drying by air, poly(methyl methacrylate) (PMMA) with a gradient microstep and nanonipple structure was obtained.

Scanning Electron Microscopy. All of the cellular morphology and structure of the samples were studied by a high-resolution scanning electron microscope (SEM, Nova NanoSEM 450) after being sputtered with Au nanoparticles. Before SEM observation, the breast cancer cells cultured on the AAO were fixed in a 2% glutaraldehyde solution for 30 min, then washed with PBS three times. After dehydration gradually with 30, 50, 70, 80, 90, 95, and 100% ethanol, they were dried by Critical Point Drying (K850, Quorum).

Fluorescence Microscopy. Cell coverage percentage was studied by calculating the percentage of the cell fluorescence coverage area to the total area using ImageJ software. After the cells were cultured with the desired densities and times, the samples were fixed with 4% paraformaldehyde for 20 min and treated with 0.2% Triton X-100 for 5 min. Then, they were treated with 100 nM fluorescein-5-isothiocyanate isomer (FITC)-phalloidin for 30 min and 5 μg/mL 4′,6-diamidino-

https://doi.org/10.1021/acsomega.2c03471
ACS Omega 2022, 7, 35668−35676

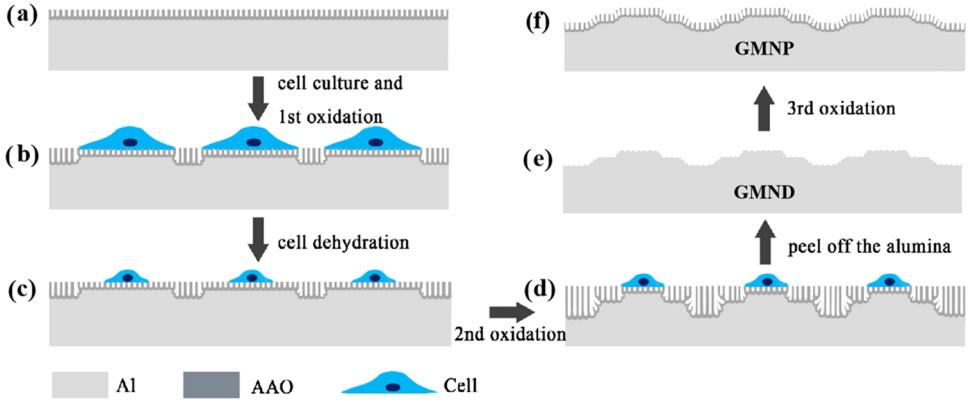

Figure 1. Schematic diagram of the preparation of AAO with a gradient microstep and nanopore structure (not to scale). (a) Ordinary self-ordered planar AAO is formed on aluminum by typical mild anodization; (b) after the top surface is cultured with the breast cancer cells, the AAO is anodized again, which is called the first anodization. New nanopores are developed at the boundaries of covered and uncovered areas. The depths of the nanopore gradually change from cell-covered areas to uncovered areas, which form microsteps with two layers at the bottom of the AAO; (c) area of the AAO covered by cells shrinks due to cell dehydration; (d) AAO cultured with cells is anodized for the second time after cell dehydration, where microsteps with three layers are formed; (e) gradient microsteps with nanodents (GMNDs) are formed on aluminum after peeling off AAO; and (f) AAO with gradient microstep and nanopores (GMNPs) is obtained after the third anodization of the prepatterned aluminum.

2-phenylindole (DAPI) for 5 min at 37 °C in the dark to stain the cytoskeleton and the nucleus respectively. The solution was rinsed with PBS three times after each step. Also, the cell fluorescence images were studied by a light microscope (DM2700, Leica).

Atomic Force Microscope (AFM). The prepared samples were cut to the proper size and fixed on the slide. Then, the samples were scanned by AFM (Nano Wizard UltraSpeed, JPK Instruments AG) phase imaging technique using AC mode.

Statistical Analysis. The cell coverage percentage was calculated by 10 random samples, expressed in terms of mean and standard deviation (SD). Also, the others were obtained in triplicate and expressed in terms of mean and standard deviation (SD).

RESULTS AND DISCUSSION

Figure 1 shows the process of fabricating a GMNP AAO using cell cultivation-assisted electrochemical anodization. Here, the breast cancer cell is chosen because it is a kind of widely used adhesive cell that is easy to obtain and culture, requiring no expensive culture media and complex culture process.[34] First, the breast cancer cell is cultured on the ordinary cylindrical AAO surface which is obtained by the typical mild anodization (Figure 1a). As the cell bodies block the electrolyte from entering the nanopores, the electrochemical reaction underneath the cell bodies is prevented in the first anodization. However, the alumina, where is not covered by cell, can grow at the right rate. Thus, the depth of the alumina uncovered by the cell is deeper than that of the alumina covered with the cell after the first anodization (Figure 1b). Then, the cultured cells on the AAO films are naturally dried at room temperature (25 °C), which results in the shrinking of the cell coverage area and exposing of new nanopores (Figure 1c). The newly exposed nanopores can grow as well as the nanopores that are not covered in the second anodization. Thus, the microsteps with three layers are formed at the bottom of AAO after the second anodization (Figure 1d). After peeling off the alumina, gradient microsteps with ordered nanodents (GMNDs) are formed on aluminum (Figure 1e). At last, the prepatterned aluminum undergoes the third oxidation, giving an AAO with gradient microsteps with ordered nanopores (GMNPs) (Figure 1f).

Figure 2 shows the SEM images and the fluorescent images of the cultured cells, aluminum with GMND, GMNP AAO, and the current variation during anodization. Breast cancer cells with a density of 4×10^4 cells/cm^2 are cultured on the ordinary cylindrical AAO membrane obtained by mild anodization. After culturing for 96 h, the cells stretch and grow well on the surface of AAO because of the good biocompatibility of alumina. The cells firmly adhere to the nanopore bridge through focal adhesion and completely cover the nanopores (Figure 2a). It can be calculated from the fluorescent pictures that 76.5% of the AAO surface is covered by cells (Figure 2a). After the anodization, AAO covered with cells is put at room temperature (25 °C) for 12 h to let the cells dry naturally. It can be clearly observed that the cell shrinks after the dehydration but still firmly sits on the AAO surface, where the widest place of the cell decreases from 35.47 to 31.82 μm (Figure 2b). After the second oxidation, followed by peeling off the alumina, a three-layer microstep structure with a nanodent on aluminum can be obtained (Figure 2c). The figure of the microstep is just like the cell, and the height gradually changes from one layer to another. It can be seen from the SEM and AFM images that the nanodents cover the top surface as well as the side surface of the layer (Figure 2c). The average width difference between the first and second steps is 3.48 ± 0.3 μm, which corresponds to the shrink degree of the cell. Since some studies have shown that the period of the nanodent can affect cell growth,[35] after the introduction of the microstep structure, the effect of microstep and nanodent structures on cell growth may be a scientific problem worth studying. Then, the aluminum prepatterned by the GMND structure is anodized for the third time to obtain the AAO with GMNP structure (Figure 2d). It also can be clearly seen that the microstep has three layers and two slopes with a height of about 2.17 ± 0.2 μm in the side view (Figure 2d). The magnified side view of GMNP shows that the nanopore can grow well on the layer surface and the slope.

https://doi.org/10.1021/acsomega.2c03471
ACS Omega 2022, 7, 35668−35676

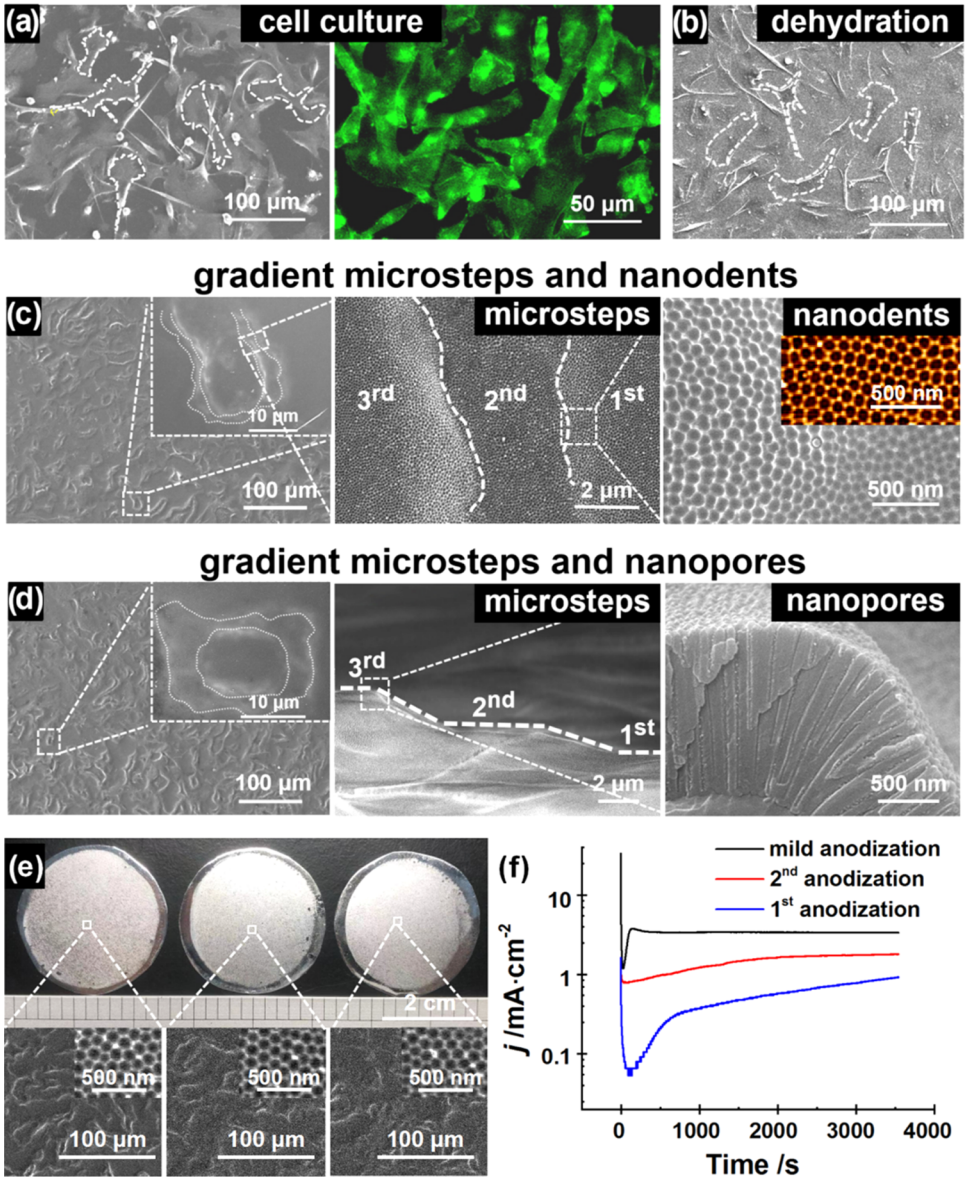

Figure 2. (a) SEM image (left) and fluorescent image (right) of cells cultured on ordinary cylindrical AAO. The white dotted lines on the SEM image show the profiles of several representative cells. (b) SEM image of dehydrated cells on AAO. The white dotted lines also show the profiles of several representative cells; (c) a series of magnified SEM images show the aluminum with a gradient microstep (left, the top right is a magnified image of one microstep with three layers), three layers of the gradient microstep with nanodents (middle) and details of the nanodents (right, the top right is an AFM image of nanodents); (d) a series of magnified SEM images show that the top view (left), side views (middle), and the details of the side view (right) of GMNP AAO. The top right is a magnified image of one microstep with three layers; (e) macroscopic optical images (top row) and the corresponding SEM images (bottom row) of the as-prepared samples obtained from different batches but the same cell culture and electrochemical oxidation conditions. The top right on the bottom row is the magnified images of the nanodent structure; and (f) current−time transients during ordinary cylindrical AAO formation by mild anodization (black color) and during cell-assisted first anodization (blue) and second anodization (red).

Here, we indeed cannot make two samples having the same gradient microstep profile because the biological cells have diversities in shape, size, growth pattern, etc., but we can make samples having identical gradient microstep distributions from the statistical view if we culture the same cell lines under the same cell culture conditions. To show the reproducibility of our method, we showed three optical images of the as-prepared macroscopic samples that are obtained from different batches but same cell culture and electrochemical oxidation conditions in Figure 2e. It can be seen from their corresponding SEM images that both the structures of the gradient microsteps and nanodents are identical. The density of the microsteps on the three samples are 1.58×10^5, 1.56×10^5, and $1.55 \times 10^5/cm^2$. Also, the average width differences between the first and second steps are 3.51 ± 0.49, 3.26 ± 0.36, and 3.33 ± 0.52 μm, respectively. It can be seen from their corresponding SEM images that both the structures of gradient microsteps and nanodents are identical.

To have a deep insight into the GMNP formation, we investigate the current density (j) variation with the anodization time in the first (first anodization) and second (second anodization), and j variation in the typical mild anodization is also recorded for comparison (Figure 2f). Here, the samples are all anodized under the same electrochemical

https://doi.org/10.1021/acsomega.2c03471
ACS Omega 2022, 7, 35668−35676

conditions. It can be seen that, in the mild anodization, j (black line) can be divided into three stages: (I), j quickly decreases from the high initial value to the lowest value of 1.3 mA/cm^2 at the beginning, which means the formation of the barrier layer; (II), then j slowly increases to the peak value of 4.3 mA/cm^2, which means the development of nanopores; and (III), j decreases and maintains a stable value of 3.8 mA/cm^2, which means the steady growth of the nanopores.[22] Like the mild anodization, j in the first (blue line) and second oxidation (red line) also decrease in the beginning. However, there are two distinct differences with that in mild anodization: (1) j in the first and second anodization is apparently lower than that in the steady anodization stage in mild anodization, and j in the second anodization is higher than that in the first anodization. (2) j always keeps on increasing after dropping to the lowest value of 0.1 mA/cm^2 in the first anodization and 0.9 mA/cm^2 in the second anodization. These phenomena are very similar to that in the anodization of Al-containing silicon imprinting.[25,27] Since most surface of the alumina is covered by the cell in the first anodization, the vertical pore growth is blocked,[27] which leads to the low current density. As more surface is exposed in the second anodization, j became higher than that in the first anodization but still lower than that in the mild anodization. However, the nanopores have an interior tendency to enlarge themselves, which is restrained by the repulsive forces from their neighboring pores during the anodization process.[36,37] Also, the alumina needs to maintain a constant porosity at a matched voltage.[35] In our case, the growth of the nanopores covered by cells is prevented, which cannot provide the repulsive forces. Thus, the pores near the boundaries tend to be larger, where new pores develop and grow vertically to the newly exposed aluminum surface to maintain a constant porosity, which leads to the continuous growth of the j in the first and second anodization.[36] As a result, the GMNP AAO, which has a larger porosity than that of the typical planar AAO, is obtained.

Obviously, cell culture density and cell culture time should play important roles to control the structure parameters of the microstep. Figure 3 shows SEM images of GMND obtained by peeling off the formed alumina after the second anodization, where the AAO is cultured with different densities cells of 2 × 10^4/cm^2 (Figure 3a), 3 × 10^4/cm^2 (Figure 3b), 4 × 10^4/cm^2 (Figure 3c), and 6 × 10^4/cm^2 (Figure 3d). The right top is the corresponding fluorescent pictures of the cultured cells on AAO, where the cell coverage percentage on the AAO film can be calculated. As the cell density increases from 2 × 10^4 to 6 × 10^4/cm^2, the cell coverage percentage increases from 12 to 93.6% (Figure 3e). However, the cell size has no obvious difference (Figure 3a–d). When the cell culture density is 2 × 10^4/cm^2, the number of microsteps is very few due to the little quantities of the cells (Figure 3a). When the culture density is 4 × 10^4/cm^2, the cells have enough space to grow and individually contract after drying. After anodization, GMND with appropriate distribution density is formed (Figure 3c). When the cell culture density is 6 × 10^4/cm^2, the cells have completely covered the surface of the nanostructure, which results in the cells blocking most of the surface from interacting with the electrolyte, and the first step cannot occur after the first anodization. In addition, the cells are so tightly contacted that they contract as a whole after dehydration, thus the second steps are not evenly distributed (Figure 3d).

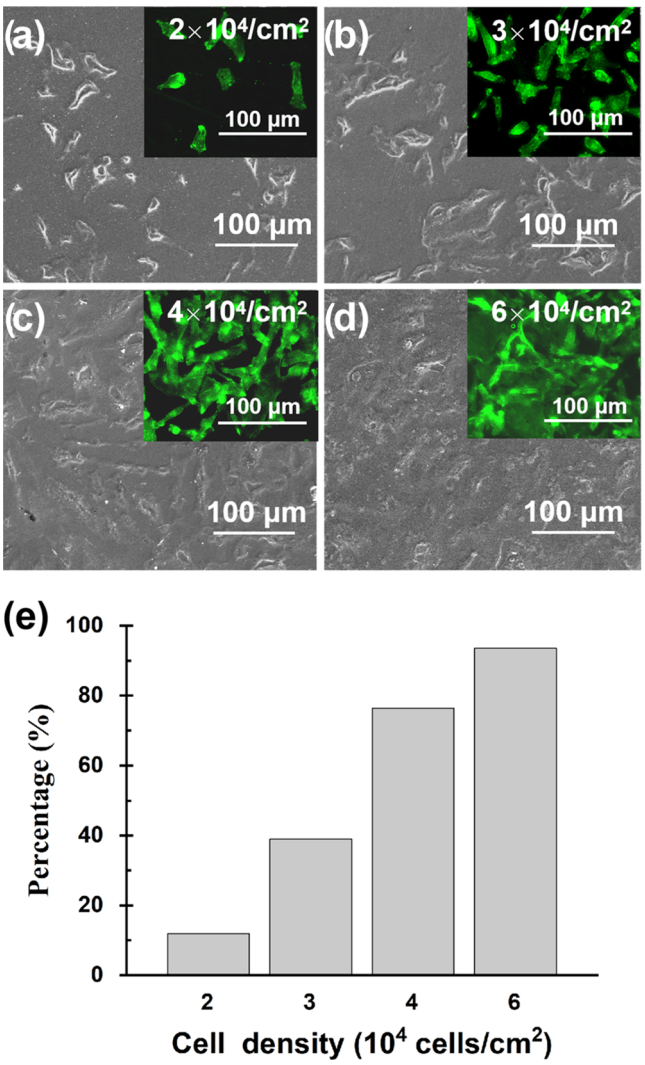

Figure 3. SEM images of GMND at different cell culture densities. (a–d) SEM images of microstep with nanodent structure obtained by peeling off the formed alumina after the second anodization, where the cells on AAO are cultured with different densities of 2 × 10^4/cm^2 (a), 3 × 10^4/cm^2 (b), 4 × 10^4/cm^2 (c), and 6 × 10^4/cm^2 (d). The right top is the corresponding fluorescent pictures of the cultured cells. (e) Cell coverage percentage under different cell culture densities.

Figure 4 shows the distribution of a microstep with nanodent structure obtained by peeling off the formed alumina after the second anodization, where the cell with a density of 4 × 10^4/cm^2 is cultured on AAO for 24 h (Figure 4a), 48 h (Figure 4b), 96 h (Figure 4c), and 120 h (Figure 4d). The right top is the corresponding fluorescent pictures of the cells cultured on AAO. It is found that only the cell number increases as the cell culture time prolongs (Figure 4e), and there is no difference in terms of the cell size. The cell coverage percentage increases from 47.9% of 24 h to 95.9% of 120 h (Figure 4e). Similar to the culture density, when the percentage is too high, the first step of the microstep gradient cannot be formed because the cells block most of the surface from interacting with the electrolyte, and the second layer of the microstep gradient cannot be formed evenly because cells cannot contract individually.

After the first oxidation, the cells grown on AAO undergo dehydration and the area of the nanopores covered with cells

https://doi.org/10.1021/acsomega.2c03471
ACS Omega 2022, 7, 35668–35676

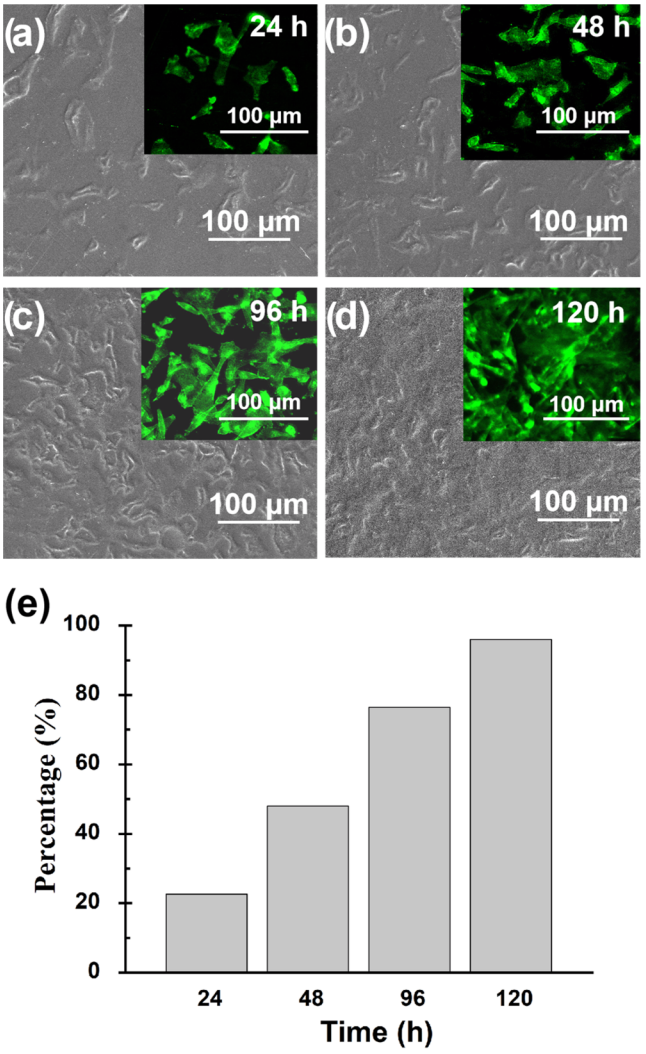

Figure 4. SEM images of GMND at different cell culture times. (a–d) SEM images of the AAO with a microstep with nanodent structure obtained by peeling off the formed alumina after the second anodization, where the cells on AAO are cultured for 24 h (a), 48 h (b), 96 h (c), and 120 h (d). The right top is the corresponding fluorescent pictures of the cultured cells. (e) Cell coverage percentage under different cell culture times.

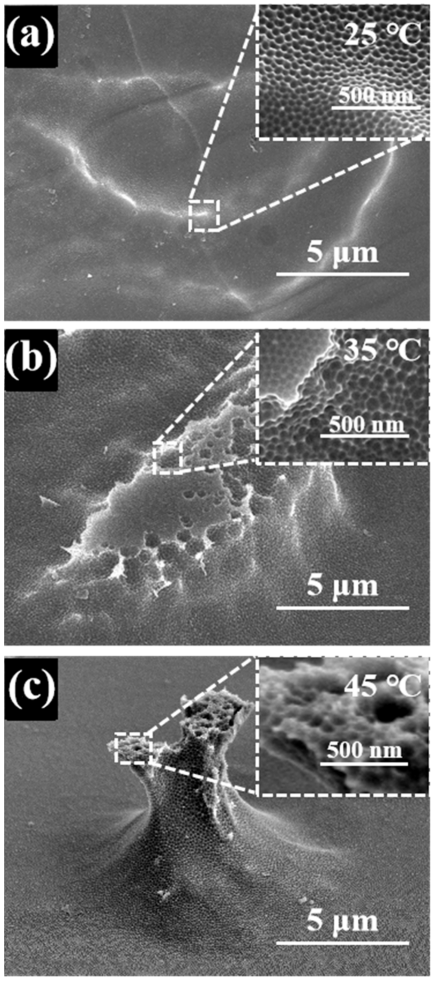

Figure 5. (a–c) SEM images of aluminum with a gradient microstep and nanodent structure obtained by peeling off the formed alumina after the second anodization, where the cells on AAO are dehydrated at 25 °C (a), 35 °C (b), and 45 °C (c). The top right shows the detail of the nanodents corresponding to the dehydration temperature.

decreases. The area in the second anodization is different from that in the first anodization, which results in the formation of a new microstep structure between the two anodizations. Thus, the cell dehydration temperature should also influence the structure of the microstep. Figure 5 shows the SEM images of a gradient microstep and nanodent structure obtained by peeling off the formed alumina after the second anodization, where the cells on AAO dehydrate at 25 °C (Figure 5a), 35 °C (Figure 5b), and 45 °C (Figure 5c). After the cells are slowly dehydrated at room temperature of 25 °C for 12 h, the gradient microstep is smooth and full (Figure 5a). After drying at 35 °C, it is difficult to maintain the integrity of the whole cell due to the acceleration of cell contraction, so the edge of the gradient structure formed is uneven. In the cell body part, the gap caused by the rapid contraction exposes the new anodization area, and thus there some pits scattered in the center of the microstep structure (Figure 5b). Interestingly, at 45 °C, an hourglass-like micro–nano-composite structure is formed after the second anodization. That is because the cells rapidly dehydrate at high temperatures and quickly shrink into a small group (Figure 5c).

The as-prepared AAO can be used as a template to fabricate a gradient microstep and nanostructure made of various materials. Figure 6a shows the process of preparing the gradient microstep and nanonipple structured poly(methyl methacrylate) (PMMA) by thermal polymerization (details can be seen in the Experiment and Method section).[38] Figure 6b shows the SEM image of AAO with a gradient microstep and tapered nanopore structure, which is fabricated by cell-assisted anodization combined with multistep mild anodization and etching.[39] Tapered nanopores on a microstep with three layers are shown on the magnified oblique view (Figure 6b). The fabricated polymer structure shows the same morphology as the AAO, except that the microsteps form a hole not a protuberance. It can be seen that nanonipples cover both the layer surface and the slop between each layer (Figure 6c). Figure 6d shows the haze effect of the polymer plate. It shows that "*snnu*" identification can be clearly seen in the flat plates. However, due to the high scattering performance of the micro–nano-composite structure, the "*snnu*" identification can

https://doi.org/10.1021/acsomega.2c03471
ACS Omega 2022, 7, 35668–35676

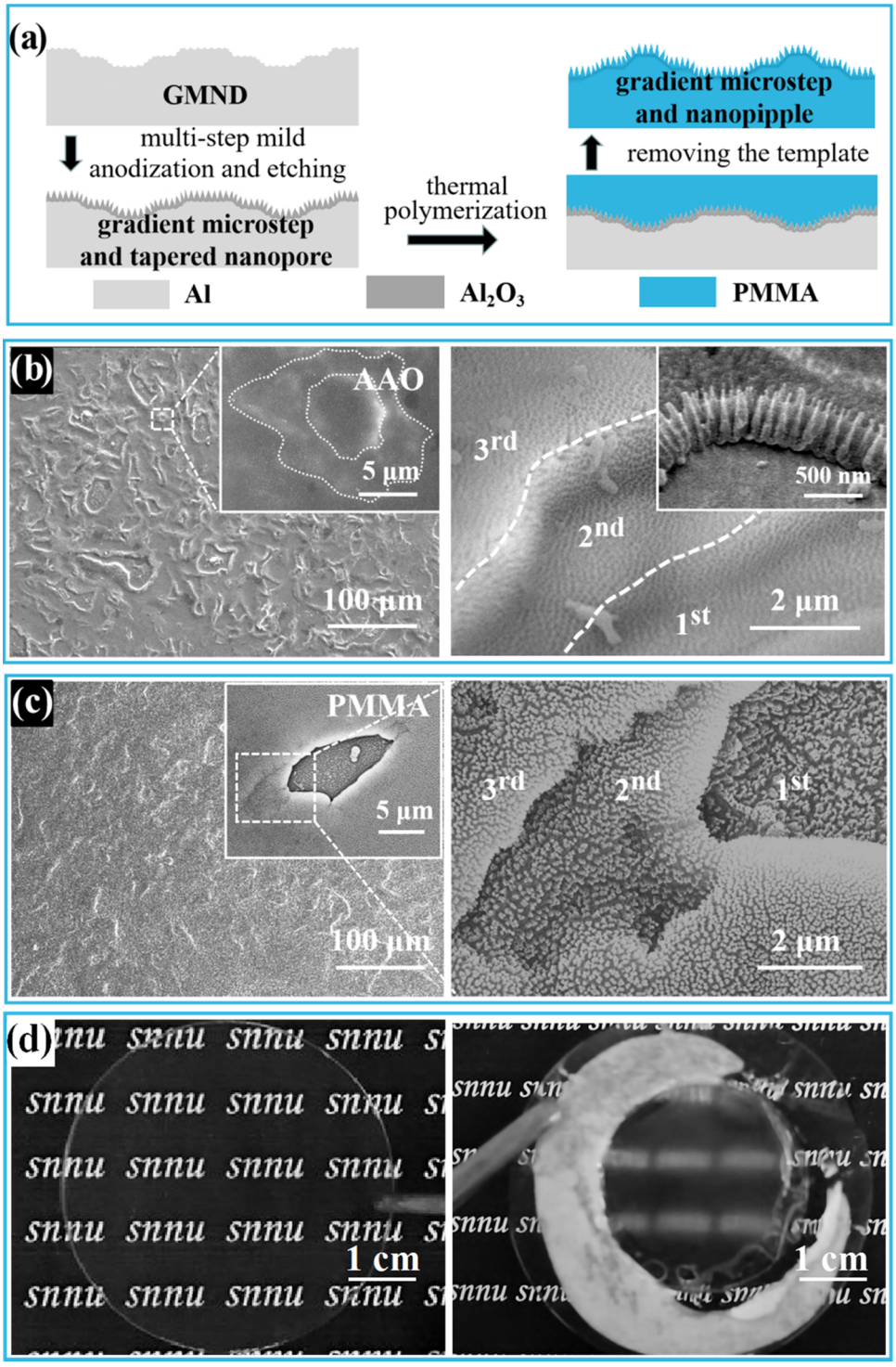

Figure 6. (a) Schematic diagram of preparing polymer with a gradient microstep and nanonipple structure. (b) SEM top view (left) and oblique view (right) of AAO with a gradient microstep and tapered nanopore structure. The right top is the magnified gradient microstep and side-view detail of the tapered nanopore structure. (c) Top-view SEM images (left) of polymer gradient microstep and the details of the nanonipple structure (right). The top right is the magnified image of one polymer microstep structure. (d) Photographic images of polymer with a gradient microstep and nanonipple structure (right) and the flat polymer plate (left) for comparison.

hardly be observed in the gradient microstep and nanonipple structured polymer plate.

CONCLUSIONS

We have demonstrated that GMNP AAO, which shows much more porosity than the typical planar AAO, can be fabricated by inversely using the cell culture to control the contact area between the alumina membrane and the electrolyte. The density of the microsteps can be adjusted by cell culture density or culture time. The figure of the microstep is influenced by cell dehydration temperature, which controls the cell shrinkage degree. The feasibility of using the GMNP

https://doi.org/10.1021/acsomega.2c03471
ACS Omega 2022, 7, 35668−35676

AAO as a template is proved by the fabricated polymer structure. It only needs simple and inexpensive apparatuses, which opens the door to the fabrication of gradient microstep and nanostructure that is made up of metal, inorganic, and polymer materials to explore novel interfacial properties.[40]

AUTHOR INFORMATION

Corresponding Authors

Juan Li − *School of Physics and Information Technology, Shaanxi Normal University, Xi'an 710119, P. R. China*; orcid.org/0000-0002-7453-9813; Email: jli2007@snnu.edu.cn

Runguang Sun − *School of Physics and Information Technology, Shaanxi Normal University, Xi'an 710119, P. R. China*; Email: sunrunguang@snnu.edu.cn

Jun Dong − *Department of Orthopaedics, Second Affiliated Hospital of Xi'an Jiaotong University, Xi'an 710004, P. R. China*; Email: dongjun_orth@xjtu.edu.cn

Authors

Zhiying Zhang − *School of Physics and Information Technology, Shaanxi Normal University, Xi'an 710119, P. R. China*

Yiyan Guo − *School of Physics and Information Technology, Shaanxi Normal University, Xi'an 710119, P. R. China*

Jiangbo Lu − *School of Physics and Information Technology, Shaanxi Normal University, Xi'an 710119, P. R. China*

Yingjun Ma − *School of Science, Ningxia Medical University, Yinchuan 750004, P. R. China*

Ting Liu − *School of Physics and Information Technology, Shaanxi Normal University, Xi'an 710119, P. R. China*

Ruiqing Liang − *School of Physics and Information Technology, Shaanxi Normal University, Xi'an 710119, P. R. China*

Complete contact information is available at: https://pubs.acs.org/10.1021/acsomega.2c03471

Author Contributions

Z.Z. contributed to the investigation, writing of the original draft and review and editing of the manuscript. Y.G. contributed to the investigation. Z.Z. and J.L. coordinated the data analysis, discussion, and review of the manuscript. J.L. contributed to the design of the experiment, supervision, review and editing of the manuscript, and funding acquisition. Y.M., T.L., and R.L fabricated the samples and characterization. R.S. contributed to the supervision and review and editing of the manuscript. J.D. contributed to the supervision and funding acquisition.

Notes

The authors declare no competing financial interest.

ACKNOWLEDGMENTS

This work was supported by the National Natural Science Foundation of China (21965030) and the Natural Science Foundation of Shaanxi Province (2020JM-287, 2020SF-190). The authors also thank the Electron Microscopy Platform of the College of Physics and Information Technology, Shaanxi Normal University, Xi'an, China.

REFERENCES

(1) Wang, Q.; Yao, X.; Liu, H.; Quéré, D.; Jiang, L. Self-Removal of Condensed Water on the Legs of Water Striders. *Proc. Natl. Acad. Sci. U.S.A.* **2015**, *112*, 9247−9252.

(2) Liu, J.; Guo, H.; Zhang, B.; Qiao, S.; Shao, M.; Zhang, X.; Feng, X. Q.; Li, Q.; Song, Y.; Jiang, L.; Wang, J. Guided Self-Propelled Leaping of Droplets on a Micro-Anisotropic Superhydrophobic Surface. *Angew. Chem., Int. Ed.* **2016**, *55*, 4265−4269.

(3) Li, Q.; Li, L.; Shi, K.; Yang, B.; Wang, X.; Shi, Z.; Tan, D.; Meng, F.; Liu, Q.; Hu, S.; Lei, Y.; Liu, S.; Xue, L. Reversible Structure Engineering of Bioinspired Anisotropic Surface for Droplet Recognition and Transportation. *Adv. Sci.* **2020**, *7*, No. 2001650.

(4) Zou, R.; Wang, J.; Tang, J.; Zhang, X.; Zhang, Y. Directionally Guided Droplets on a Modular Bottom-Up Anisotropic Locally Ordered Nickel Nanocone Superhydrophobic Surface. *ACS Appl. Mater. Interfaces* **2021**, *13*, 13848−13860.

(5) Feng, S.; Delannoy, J.; Malod, A.; Zheng, H.; Quéré, D.; Wang, Z. Tip-Induced Flipping of Droplets on Janus Pillars: From Local Reconfiguration to Global Transport. *Sci. Adv.* **2020**, *6*, No. eabb4540.

(6) Wang, X.; Zeng, J.; Li, J.; Yu, X.; Wang, Z.; Zhang, Y. Beetle and Cactus-Inspired Surface Endows Continuous and Directional Droplet Jumping for Efficient Water Harvesting. *J. Mater. Chem. A* **2021**, *9*, 1507−1516.

(7) Zhu, T.; Cheng, Y.; Huang, J.; Xiong, J.; Ge, M.; Mao, J.; Liu, Z.; Dong, X.; Chen, Z.; Lai, Y. A Transparent Superhydrophobic Coating with Mechanochemical Robustness for Anti-Icing, Photocatalysis and Self-Cleaning. *Chem. Eng. J.* **2020**, *399*, No. 125746.

(8) Park, J.; Kim, D. H.; Kim, H. N.; Wang, C. J.; Kwak, M. K.; Hur, E.; Suh, K. Y.; An, S. S.; Levchenko, A. Directed Migration of Cancer Cells Guided by the Graded Texture of the Underlying Matrix. *Nat. Mater.* **2016**, *15*, 792−801.

(9) Kim, D. H.; Han, K.; Gupta, K.; Kwon, K. W.; Suh, K. Y.; Levchenko, A. Mechanosensitivity of Fibroblast Cell Shape and Movement to Anisotropic Substratum Topography Gradients. *Biomaterials* **2009**, *30*, 5433−5444.

(10) Wang, D.; Sun, Q.; Hokkanen, M. J.; Zhang, C.; Lin, F. Y.; Liu, Q.; Zhu, S. P.; Zhou, T.; Chang, Q.; He, B.; Zhou, Q.; Chen, L.; Wang, Z.; Ras, R. H. A.; Deng, X. Design of Robust Superhydrophobic Surfaces. *Nature* **2020**, *582*, 55−59.

(11) Long, J.; Zhou, P.; Huang, Y.; Xie, X. Enhancing the Long-Term Robustness of Dropwise Condensation on Nanostructured Superhydrophobic Surfaces by Introducing 3D Conical Microtextures Prepared by Femtosecond Laser. *Adv. Mater. Interfaces* **2020**, *7*, No. 2000997.

(12) Pan, R.; Zhang, H.; Zhong, M. Triple-Scale Superhydrophobic Surface with Excellent Anti-Icing and Icephobic Performance via Ultrafast Laser Hybrid Fabrication. *ACS Appl. Mater. Interfaces* **2021**, *13*, 1743−1753.

(13) Losic, D.; Santos, A.*Nanoporous Alumina: Fabrication, Structure, Properties and Applications*; Springer International Publishing, 2015.

(14) Lee, W.; Park, S. J. Porous Anodic Aluminum Oxide: Anodization and Templated Synthesis of Functional Nanostructures. *Chem. Rev.* **2014**, *114*, 7487−7556.

(15) Md Jani, A. M.; Losic, D.; Voelcker, N. H. Nanoporous Anodic Aluminium Oxide: Advances in Surface Engineering and Emerging Applications. *Prog. Mater. Sci.* **2013**, *58*, 636−704.

(16) Masuda, H.; Fukuda, K. Ordered Metal Nanohole Arrays Made by a Two-Step Replication of Honeycomb Structures of Anodic Alumina. *Science* **1995**, *268*, 1466−1468.

(17) Lee, W.; Ji, R.; Gösele, U.; Nielsch, K. Fast Fabrication of Long-Range Ordered Porous Alumina Membranes by Hard Anodization. *Nat. Mater.* **2006**, *5*, 741−747.

(18) Lee, W.; Ji, R.; Ross, C. A.; Gösele, U.; Nielsch, K. Wafer-Scale Ni Imprint Stamps for Porous Alumina Membranes Based on Interference Lithography. *Small* **2006**, *2*, 978−982.

(19) Mebed, A. M.; Abd-Elnaiem, A. M.; El-Said, W. A.; Asafa, T. B. Review on the Formation of Anodic Metal Oxides and their Sensing Applications. *Curr. Nanosci.* **2018**, *15*, 6−21.

(20) Zajączkowska, L.; Siemiaszko, D.; Norek, M. Towards Self-Organized Anodization of Aluminium in Malic Acid Solutions-New

https://doi.org/10.1021/acsomega.2c03471
ACS Omega 2022, 7, 35668−35676

Aspects of Anodization in the Organic Acid. *Materials* **2020**, *13*, No. 3899.
(21) Zajączkowska, L.; Norek, M. Peculiarities of Aluminum Anodization in AHAs-Based Electrolytes Case Study of the Anodization in Glycolic Acid Solution. *Materials* **2021**, *14*, No. 5362.
(22) Ma, Y.; Wen, Y.; Li, J.; Li, Y.; Zhang, Z.; Feng, C.; Sun, R. Fabrication of Self-Ordered Alumina Films with Large Interpore Distance by Janus Anodization in Citric Acid. *Sci. Rep.* **2016**, *6*, No. 39165.
(23) Banerjee, S.; Myung, Y.; Banerjee, P. Confined Anodic Aluminum Axide Nanopores on Aluminum Wires. *RSC Adv.* **2014**, *4*, 7919−7926.
(24) Vanpaemel, J.; Abd-Elnaiem, A. M.; Gendt, S. D.; Vereecken, P. M. The Formation Mechanism of 3D Porous Anodized Aluminum Oxide Templates from an Aluminum Film with Copper Impurities. *J. Phys. Chem. C* **2015**, *119*, 2105−2112.
(25) Abd-Elnaiem, A. M.; Mebed, A. M.; Gaber, A.; Abdel-Rahim, M. A. Tailoring the Porous Nanostructure of Porous Anodic Alumina Membrane with the Impurity Control. *J. Alloys Compd.* **2016**, *659*, 270−278.
(26) Mebed, A. M.; Abd-Elnaiem, A. M.; Al-Hosiny, N. M. Electrochemical Fabrication of 2D and 3D Nickel Nanowires Using Porous Anodic Alumina Templates. *Appl. Phys. A* **2016**, *122*, No. 565.
(27) Abd-Elnaiem, A. M.; Mebed, A. M.; Alamri, H. R.; Assaedi, H. S. Tailoring Controllable Nanowire Morphologies Using a Multilayer Porous Anodic Alumina Template for Technological Applications. *J. Electrochem. Soc.* **2020**, *167*, No. 103505.
(28) Thompson, G. E. Porous Anodic Alumina: Fabrication, Characterization and Applications. *Thin Solid Films* **1997**, *297*, 192−201.
(29) Rajeev, G.; Simon, B. P.; Marsal, L. F.; Voelcker, N. H. Advances in Nanoporous Anodic Alumina-Based Biosensors to Detect Biomarkers of Clinical Significance: A Review. *Adv. Healthcare Mater.* **2018**, *7*, No. 1700904.
(30) Brüggemann, D. Nanoporous Aluminium Oxide Membranes as Cell Interfaces. *J. Nanomater.* **2013**, *2013*, 1−18.
(31) Nasrollahi, S.; Banerjee, S.; Qayum, B.; Banerjee, P.; Pathak, A. Nanoscale Matrix Topography Influences Microscale Cell Motility through Adhesions, Actin Organization, and Cell Shape. *ACS Biomater. Sci. Eng.* **2017**, *3*, 2980−2986.
(32) Kim, S.; Han, D. Y.; Chen, Z.; Lee, W. G. Dependence of Cell Adhesion on Extracellular Matrix Materials Formed on Pore Bridge Boundaries by Nanopore Opening and Closing Geometry. *Analyst* **2018**, *143*, 2141−2149.
(33) Park, J. S.; Moon, D.; Kim, J. S.; Lee, J. S. Cell Adhesion and Growth on the Anodized Aluminum Oxide Membrane. *J. Biomed. Nanotechnol.* **2016**, *12*, 575−580.
(34) Mo, R.; Jiang, T.; DiSanto, R.; Tai, W.; Gu, Z. ATP-Triggered Anticancer Drug Delivery. *Nat. Commun.* **2014**, *5*, No. 3364.
(35) Cho, W. K.; Kang, K.; Kang, G.; Jang, M. J.; Nam, Y.; Cho, I. S. Pitch-Dependent Acceleration of Neurite Outgrowth on Nanostructured Anodized Aluminum Oxide Substrates. *Angew. Chem., Int. Ed.* **2010**, *49*, 10114−10118.
(36) Su, Z.; Hähner, G.; Zhou, W. Investigation of the Pore Formation in Anodic Aluminium Oxide. *J. Mater. Chem.* **2008**, *18*, 5787−5795.
(37) Ono, S.; Saito, M.; Asoh, H. Self-Ordering of Anodic Porous Alumina Formed in Organic Acid Electrolytes. *Electrochim. Acta* **2005**, *51*, 827−833.
(38) Feng, C.; Zhang, Z.; Li, J.; Qu, Y.; Xing, D.; Gao, X.; Zhang, Z.; Wen, Y.; Ma, Y.; Ye, J.; Sun, R. A Bioinspired, Highly Transparent Surface with Dry-Style Antifogging, Antifrosting, Antifouling, and Moisture Self-Cleaning Properties. *Macromol. Rapid Commun.* **2019**, *40*, No. 1800708.
(39) Du, K.; Gan, Z. Cellular Interactions on Poly (ε-caprolactone) Nanowire Micropatterns. *ACS Appl. Mater. Interfaces* **2012**, *4*, 4643−4650.
(40) Liu, M.; Wang, S.; Jiang, L. Nature-Inspired Superwettability Systems. *Nat. Rev. Mater.* **2017**, *2*, No. 17036.

https://doi.org/10.1021/acsomega.2c03471
ACS Omega 2022, 7, 35668−35676